© 2016. Published by The Company of Biologists Ltd | Development (2016) 143, 2541-2547 doi:10.1242/dev.137000

RESEARCH REPORT

Roles of Wnt pathway genes *wls*, *wnt9a*, *wnt5b*, *frzb* and *gpc4* in regulating convergent-extension during zebrafish palate morphogenesis

Lucie Rochard[1], Stefanie D. Monica[2], Irving T. C. Ling[1], Yawei Kong[1], Sara Roberson[3], Richard Harland[2], Marnie Halpern[3] and Eric C. Liao[1,*]

ABSTRACT

The Wnt signaling pathway is crucial for tissue morphogenesis, participating in cellular behavior changes, notably during the process of convergent-extension. Interactions between Wnt-secreting and receiving cells during convergent-extension remain elusive. We investigated the role and genetic interactions of Wnt ligands and their trafficking factors Wls, Gpc4 and Frzb in the context of palate morphogenesis in zebrafish. We describe that the chaperon Wls and its ligands Wnt9a and Wnt5b are expressed in the ectoderm, whereas juxtaposed chondrocytes express Frzb and Gpc4. Using *wls*, *gpc4*, *frzb*, *wnt9a* and *wnt5b* mutants, we genetically dissected the Wnt signals operating between secreting ectoderm and receiving chondrocytes. Our analysis delineates that non-canonical Wnt signaling is required for cell intercalation, and that *wnt5b* and *wnt9a* are required for palate extension in the anteroposterior and transverse axes, respectively.

KEY WORDS: Wnt, Convergent-extension, Zebrabow, Palate, Morphogenesis

INTRODUCTION

Wnt signaling is a key pathway regulating tissue morphogenesis, notably through its role in the process of convergent-extension (CE), whereby cells medialize and intercalate in one axis with concurrent extension in the perpendicular direction (Gray et al., 2011; Heisenberg and Tada, 2002; Heisenberg et al., 2000; Topczewski et al., 2011; Tudela et al., 2002; Wallingford et al., 2002; Westfall et al., 2003; Yin et al., 2009). The zebrafish ethmoid plate (hereafter palate) forms by the convergence and the integration of the midline frontonasal and paired maxillary prominences (Geetha-Loganathan et al., 2009; Kamel et al., 2013; Dougherty et al., 2013; Topczewski et al., 2001; Szabo-Rogers et al., 2010). The Wnt planar cell polarity (PCP) pathway has been implicated in both CE and craniofacial development but how it regulates cell behavior during palate morphogenesis remains elusive (Kibar et al., 2007; Sisson et al., 2015; Szabo-Rogers et al., 2010; Yang et al., 2014; Yin et al., 2009; Yu et al., 2010).

[1]Center for Regenerative Medicine, Massachusetts General Hospital, Harvard Medical School, Harvard Stem Cell Institute, Boston, MA 02114, USA. [2]Department of Molecular and Cell Biology, University of California Berkeley, Berkeley, CA 94720, USA. [3]Department of Embryology, Carnegie Institution for Science, and Department of Biology, Johns Hopkins University, 3520 San Martin Drive, Baltimore, MD 21218, USA.

*Author for correspondence (cliao@partners.org)

E.C.L., 0000-0003-3989-5115

Received 2 March 2016; Accepted 23 May 2016

Wnts are highly conserved secreted proteins that share a common secretion factor, Wntless (Wls), which is a multi-pass transmembrane protein that transports Wnt from the Golgi apparatus to the cell membrane (Bartscherer and Boutros, 2008; Brugmann et al., 2007; Franch-Marro et al., 2008; Garcia-Castro et al., 2002; Gleason et al., 2006; Harterink and Korswagen, 2012; Lee et al., 2008; Najdi et al., 2012; Wodarz and Nusse, 1998). Wnts show high hydrophobicity, which limits their free diffusion in the extracellular space. Extracellular matrix components, such as Glypican (Gpc4), ensure their diffusion to neighboring cells, while sFRP (Frzb) enhances diffusion of Wnt by blocking short-range effects and increasing long-range gene responses (Cadigan and Peifer, 2009; Gallet et al., 2008). At the receiving cell surface, Wnts bind to their receptor Frizzled (Fzd), activating an intracellular cascade of canonical β-catenin or non-canonical pathways (Chiquet et al., 2008; Clevers, 2006; He and Chen, 2012; Zecca et al., 1996).

We carried out morphogenetic analyses of the Wnt pathway from the epithelium (signaling cell) to the chondrocyte (recipient cell) during palate development in zebrafish. We analyzed the requirement of genes encoding Wnt ligands (Wnt9a and Wnt5b), proteins involved in secretion (Wls) and extracellular Wnt localization (Frzb and Gpc4). We detailed the relative contribution of each Wnt component to cellular behaviors mediating palate morphogenesis.

RESULTS AND DISCUSSION

Requirement of Wnt pathway genes in palate morphogenesis

We previously showed that *wnt9a* is expressed in the oropharyngeal epithelium, whereas *frzb* is expressed in the distal chondrocytes of the palate (Dougherty et al., 2013; Kamel et al., 2013). Consistent with the requirement for Wnt secretion, *wls* is expressed in the epithelial and mesenchymal tissues surrounding the palate, colocalized with *wnt9a* (Fig. S1A,F,K, black arrowheads; Fig. S1D,I,N, black and open arrowheads in N), and overlapping with *wnt5b* in the epithelium lining the mouth opening (Fig. S1A,F,K, open arrowhead; Fig. S1E,J,O, black arrowheads in E and O). *gpc4* is expressed more broadly, in both chondrocytes and epithelium (Fig. S1B, black arrowhead; Fig. S1G,L).

To elucidate the requirement of Wnt genes in palate morphogenesis, *wls* (*c186* allele) (Kuan et al., 2015), *gpc4* (*knypek*) (Topczewski et al., 2001) and *wnt5b* (*pipetail*) (Westfall et al., 2003) mutants were collected, and *frzb* and *wnt9a* mutants were generated (Hwang et al., 2013) (Fig. S2). We generated two alleles for each gene, confirming the specificity of their craniofacial phenotype. Analyses were conducted on wls^{c186}, $wnt9a^{c.116\_118del}$ and $frzb^{c.481\_487del}$ alleles. Phenotypes were assessed by Alcian Blue staining of craniofacial skeletons and by measuring palate dimensions: length (L), width (W) and L/W ratio (Fig. 1).

Development (2016) 143, 2541-2547 doi:10.1242/dev.137000

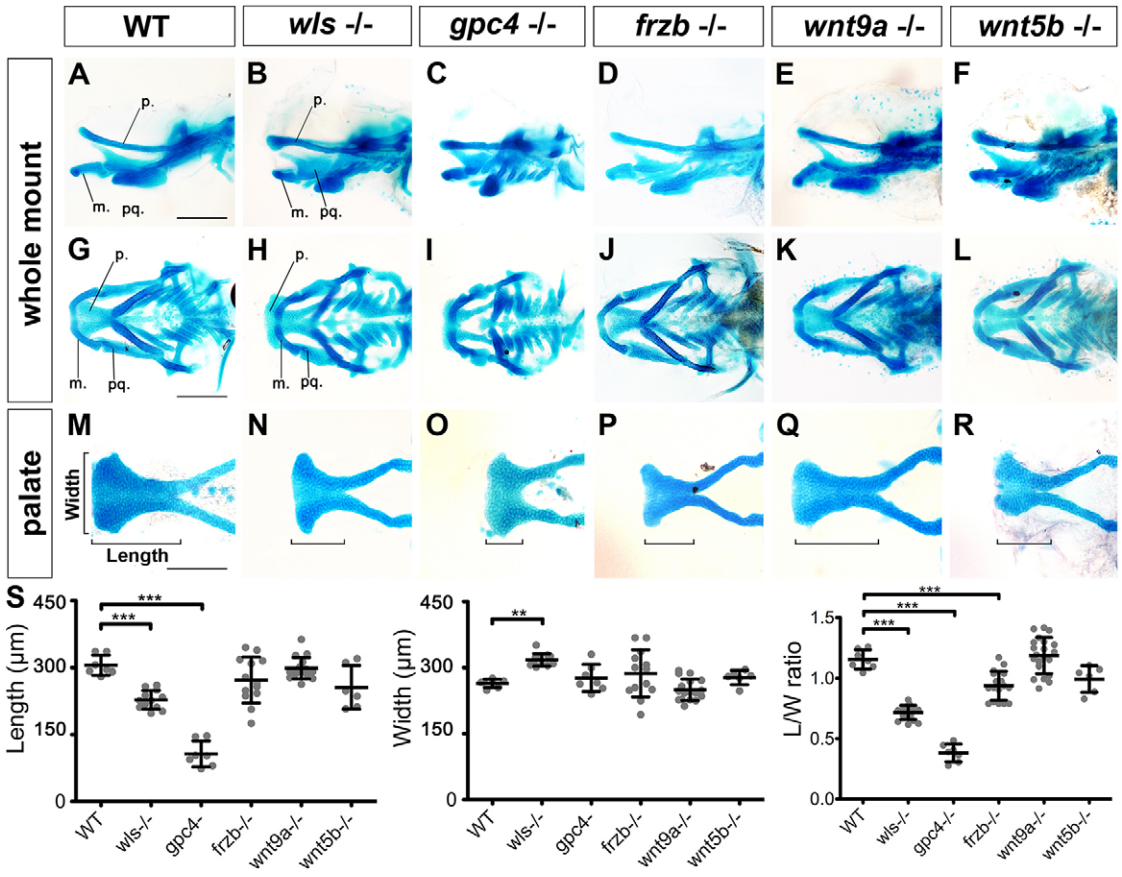

Fig. 1. Wnt signaling is required for palate morphogenesis. (A-R) Alcian Blue-stained 4.5 dpf zebrafish larvae. (A-F) Lateral, (G-L) ventral, (M-R) detailed view of dissected palate. (S) Length, width and average length/width ratio measured in WT and mutants as illustrated in M. ***P*<0.01, ****P*<0.0001. p, palate; m, Meckel's; pq, palatoquadrate.

For wild-type (WT) palate, the average L/W ratio was 1.15±0.08 (*n*=7; Fig. 1S). The *wls* mutant produced a shorter and wider palate with a L/W ratio of less than 1 (0.7±0.06, *n*=17; Fig. 1B,H,N,S). The morphology of mutant *gpc4* cartilage was similar to *wls*$^{-/-}$, although more severely dysmorphic (L/W ratio of 0.38±0.07, *n*=6; Fig. 1C,I,O,S). This was unexpected based on their function in Wnt trafficking, where Wls regulates all Wnt secretion and Gpc4 functions as a Wnt co-receptor for short-range diffusion. The greater severity of the *gpc4* mutant phenotype compared with the *wls* mutant could be the consequence of earlier embryogenesis defects, since *gpc4* mutants exhibited anomalies in body axis extension, or might be a consequence of its role in additional pathways (Filmus et al., 2008).

frzb mutants showed a discrete phenotype of slightly shortened palate (L/W ratio of 0.94±0.12, *n*=17; Fig. 1D,J,P,S), consistent with previous mouse work (Lories et al., 2007), but less severe than that observed with morpholino knockdown (Kamel et al., 2013; Dougherty et al., 2013). This difference between mutants and morphants has been reported previously as the field increasingly generates mutants, and might be explained by morpholino off-target effects or compensations that mitigate *frzb* mutation effects (Lodewyckx et al., 2012; Neumann et al., 2009; Panakova et al., 2005; Rossi et al., 2015).

Likewise, *wnt9a*$^{-/-}$ palate exhibited a modest phenotype compared with the morphant (Dougherty et al., 2013). The palate was elongated and narrower, but not significantly different from WT (L/W ratio of 1.19±0.15, *n*=21; Fig. 1Q,S). The *wnt5b* mutant showed a shorter palate than WT, but longer than *wls* mutant (Fig. 1F,L,R,S). Quantitatively, the L/W ratio was not affected (0.97±0.19, *n*=5). Consistent with their restricted expression patterns, the *wnt9a* and *wnt5b* mutant phenotypes suggest distinct requirements in palate morphogenesis. *wnt5b* is expressed in a discrete anterior domain and appears to be required for extension of the palate along the anteroposterior (AP) axis. *wnt9a* is expressed in the epithelium surrounding chondrocytes and is required in the extension of chondrocytes in the transverse axis of the palate.

Chondrocyte stacking reflects palate phenotype

Chondrocyte shape, orientation and stacking are crucial for craniofacial cartilage form and function (LeClair et al., 2009; Sisson et al., 2015; Sisson and Topczewski, 2009; Topczewski et al., 2001). Chondrocyte organization was assessed by measuring the L/W ratio (the longest cell axis measured as L, and the shorter axis as W) and the orientation as the angle between the AP axis of the palate and the longest axis of the cell. Finally, chondrocyte stacking was evaluated by the number of cell layers along the dorsoventral (DV) axis (Fig. 2Y).

In WT, chondrocytes organize as columns (Fig. 2G), oriented perpendicularly to the AP axis 90°-120°, as a single layer (Fig. 2M,S). Detailed view of mutant palates revealed significant differences in *wls*$^{-/-}$ and *gpc4*$^{-/-}$. In the *wls* mutant, chondrocytes were smaller, rounded and lacked stacking in linear columns (Fig. 2B,H). Cells were randomly oriented (35°-145°, Fig. 2N) and exhibited excessive stacking in the DV axis (Fig. 2T). Similarly, *gpc4* mutant chondrocytes showed defects in elongation and orientation and organized as a multi-layered structure (Fig. 2I,O,U).

In *frzb*$^{-/-}$, *wnt9a*$^{-/-}$ and *wnt5b*$^{-/-}$ embryos, cell orientation and stacking did not significantly differ from WT (Fig. 2P-R,V-X,Z).

Development (2016) 143, 2541-2547 doi:10.1242/dev.137000

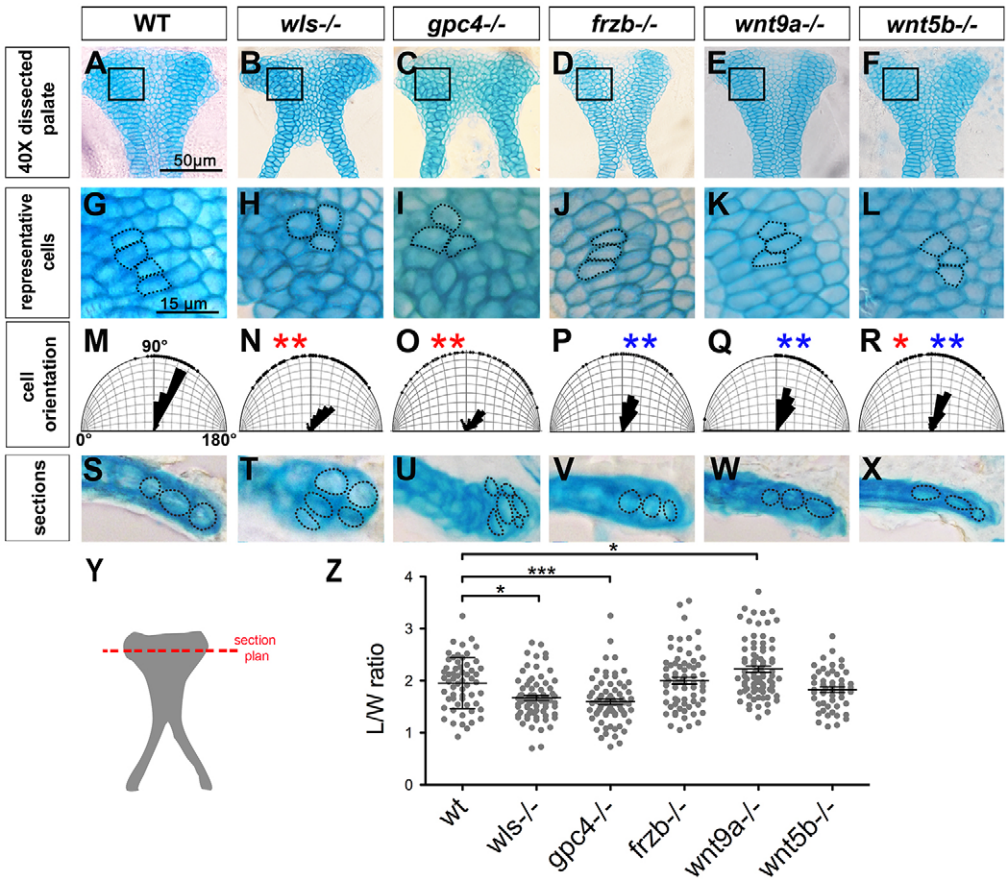

Fig. 2. Cell shape and orientation are defective in Wnt signaling mutants. (A-F) Dissected palate (anterior to the top). (G-L) Representative region (as boxed above) magnified to illustrate cell shape and organization. (M-R) Cell orientation was measured and compared with WT (significantly different indicated by red asterisk) and with *wls* mutant (significantly different indicated by blue asterisk). Watson-U^2 test. (S-X) Transverse sections (following the cut plane illustrated in Y) showing chondrocytes stacking in the DV axis. (Z) Graphic representation of the cell L/W ratio. **P*<0.05, ****P*<0.0001.

wnt9a$^{-/-}$chondrocytes exhibited a significantly increased L/W ratio (2.23±0.54 versus 1.95±0.49 for WT, Fig. 2Z) but stacked normally (Fig. 2W). *wnt5b*$^{-/-}$ exhibited smaller chondrocytes consistent with a Wnt-Ca^{2+} role in cell inflation (Hartmann and Tabin, 2000; Enomoto-Iwamoto et al., 2002). Moreover, *wnt5b* mutation affected the columnar organization but not the single layer stacking (Fig. 2L,X).

Detailed observation of *wls* mutant chondrocytes showed that Wnt signaling regulates palate morphogenesis through its effect on chondrocyte size, orientation and stacking. This analysis highlights the crucial role of Wnt-PCP, since *gpc4* mutation recapitulates most defects observed in *wls* mutants.

wls mutation affects the CE mechanism

Palate morphogenesis is mediated by the convergence and integration of facial prominences, followed by palate elongation through cell proliferation (Dougherty et al., 2013; Kamel et al., 2013). In other developmental contexts, Wnt-PCP signaling mediates the CE mechanism, driving axis elongation by cellular reorganization. To explore if a similar process is involved during palate morphogenesis under the control of Wnt, we observed cell behaviors in the *wls* mutant.

We first assessed cell proliferation using two independent methods: photoconversion cell labeling and EdU assays. As previously described, in the pulse-chase assay the photoconversion of Kaede protein, driven by the neural crest-specific *sox10* promoter, was performed. The entire distal edge of the palate was irreversibly photoconverted from green to red at 55 hpf, and the embryo was then allowed to develop and reimaged at 72 hpf. The palate is noted to have extended where the green chondrocytes are detected distally to the photoconverted region, indicating that new cells have been added along a distal front. This photoconversion assay illustrates extension of the lateral element of the palate via both proliferation and morphological changes (Fig. 3A,J) (Swartz et al., 2011; Dougherty et al., 2013; Kamel et al., 2013). In this assay, at 72 hpf WT and *wls* mutant showed comparable proliferation at the distal edge of the palate (Fig. 3B,K). Further, EdU labeling confirmed normal proliferation at the distal tip in both WT and *wls* mutant (Fig. 3C,L,Q). TUNEL assays and Acridine Orange staining did not reveal increased cell death in *wls* mutant compared with WT (not shown). Together, our data demonstrate that defects in cell proliferation and survival do not explain the shortened palate phenotype in the *wls* mutant.

Since cranial neural crest cells (NCCs) develop normally (Fig. S3) and chondrocytes survive and proliferate normally in the *wls* mutant, and the *wls* mutant palate exhibited increased cellularity in the DV axis (Fig. 2T), we examined how cell movements might be defective to give rise to the aberrant tissue architecture. We tested this hypothesis by visualizing cell rearrangements using the Zebrabow system (Pan et al., 2013; Vieira et al., 2005). The *Zebrabow* transgenic line enables labeling of clonal cell populations over time by allowing each cell and their descendants to express a unique combination of three fluorescent proteins: RFP, YFP and CFP (Livet et al., 2007; Pan et al., 2013; Rochard et al., 2015). WT *Zebrabow* palate depicted mediolateral intercalation along the AP axis (Fig. 3D-G,M-O) (Keller et al., 2008; Wallingford et al., 2002). Following the yellow clonal population, we were able to visualize CE occurring in three discrete steps (Fig. 3, from E, immature cells, to G, more mature cells): cells initially proliferate and aggregate distally at the newly formed part of the palate (Fig. 3E); cells then mature and organize into columns (Fig. 3F); and finally the chondrocytes intercalate proximally and drive elongation in the AP

Development (2016) 143, 2541-2547 doi:10.1242/dev.137000

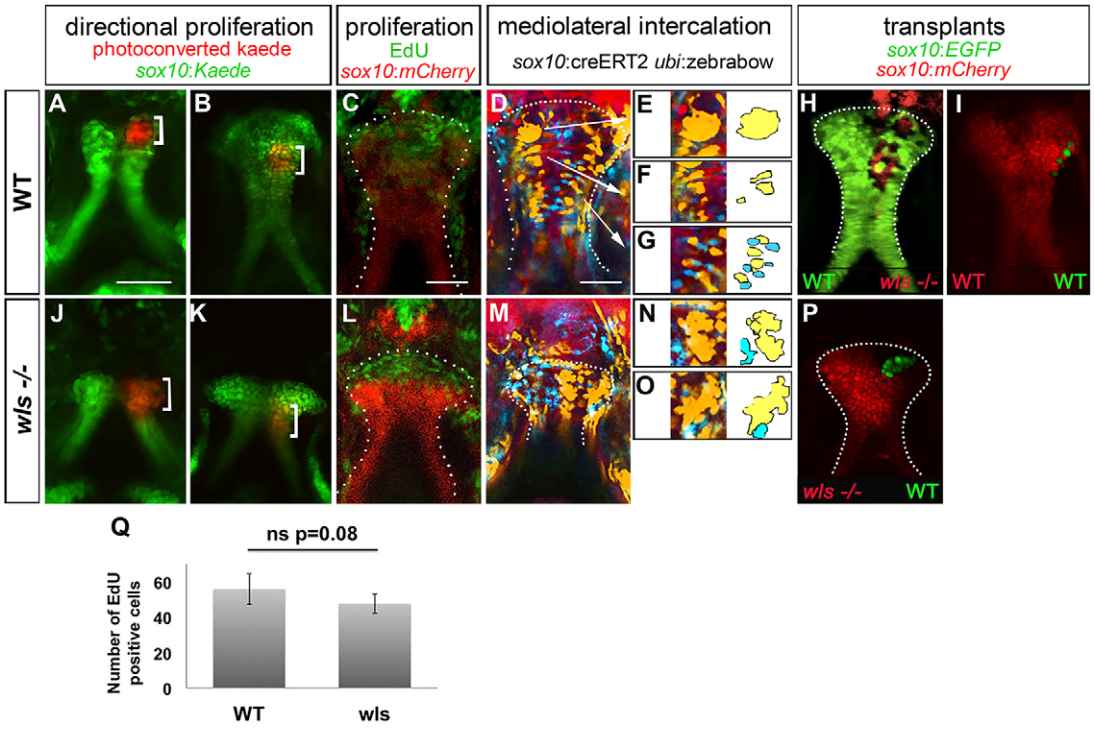

Fig. 3. Chondrocytes proliferate normally but fail to intercalate in *wls* mutants. Anterior is up in all views. (A-I) WT larvae, (J-P) *wls* mutants. Photoconverted *sox10:kaede* (red, bracket) in WT (A,B) and *wls* mutants (J,K) at 55 hpf (A,J) and 72 hpf (B,K). EdU incorporation assay in WT (C) and *wls* mutant (L). Multi-spectral clonal analysis in WT (D-G) and *wls* mutants (M-O). WT chondrocytes undergo a CE from distal to proximal, cells proliferate and group (D,E), converge into columns (D,F) and intercalate (D,G). In *wls* mutants, cells fail to undergo intercalation (M-O). Yellow and blue groups of cells are illustrated schematically to assist in visualization of the cell intercalation process. (H,I,P) Presumptive cranial NCCs were transplanted from WT *sox10:EGFP* to *wls*$^{-/-}$ *sox10:mCherry* and reciprocally. *wls* cells intercalated in 4/5 WT (H); WT cells formed groups in 5/6 mutants (P). (I) Control experiment, from WT *sox10:EGFP* to *sox10:mCherry* WT. (Q) Quantification of EdU-positive cells. Six WT and five *wls* mutant embryos were used and positive cells were counted for each. Average of number positive cells were calculated. ns, not significant (Student's *t*-test).

axis, remaining as a single cell layer sheet in the DV axis (Fig. 3G). In contrast, these cell behaviors of intercalation and extension failed to occur in the *wls* mutant, as cells remained aggregated throughout the palate, chondrocytes did not intercalate with neighboring cells, and cells extended in the AP and DV axes (Fig. 3M-O).

It is commonly accepted that Wnt acts on neighboring cells (Strigini and Cohen, 2000). Since *wls* is only expressed in surrounding epithelial and mesenchymal cells (Fig. S1), it might regulate chondrocyte intercalation from these surrounding tissues. We assessed the ability of *wls*-deficient cranial NCCs to intercalate in a WT context using cell transplantations (Kemp et al., 2009). These experiments revealed that *wls*-deficient cells behave normally in a WT host (Fig. 3H compared with 3I), as they undergo normal intercalation and spread along the AP axis. Conversely, in a *wls*$^{-/-}$ host, WT cells failed to intercalate and spread along the AP axis, remaining grouped (Fig. 3P). *wls*-deficient NCCs behave normally in a WT context, whereas WT cells cannot in the *wls* mutant background, suggesting that the cell intercalation signal is provided by surrounding Wnt-expressing epithelial tissues in a non-cell-autonomous manner.

Together, these results suggest that Wnt signaling, provided by epithelium and mesenchyme tissues surrounding chondrocytes, is required for proper cell intercalation but not for cell proliferation during palate morphogenesis.

Genetic interactions between *wls*, *gpc4*, *frzb*, *wnt9a* and *wnt5b* in the non-canonical Wnt pathway

We next sought to examine genetic interactions between the Wnt genes described above and to validate the role of PCP by generating compound mutants (Fig. 4). We hypothesized that combining *wls*$^{-/-}$ with mutants of downstream genes (*gpc4*, *frzb*, *wnt5b* and *wnt9a*) would recapitulate the *wls* mutant phenotype.

An additive effect of mutations was not observed in the *wls*$^{-/-}$;*gpc4*$^{-/-}$ compound mutant (Fig. 4C,I,O), suggesting that both genes act similarly on palate morphogenesis. The palate phenotype of the *wnt9a*$^{-/-}$;*wnt5b*$^{-/-}$ double mutant appeared to be a combination of the respective single mutants, significantly different from *wls*$^{-/-}$ but not from WT (Fig. 4F,L,R). The addition of their respective phenotypes suggests that they might function independently. *wnt9a*$^{-/-}$;*wnt5b*$^{-/-}$ did not recapitulate the *wls*$^{-/-}$ phenotype, implying that the Wnt-Ca^{2+} pathway (represented by *wnt5b*) and the Wnt9a signal are not involved in CE. Instead, this suggests the role of additional Wnt ligands, such as Wnt11 or Wnt4, in palate development (Lee et al., 2008; He and Chen, 2012).

The addition of *frzb* mutation to *wls* mutation partially rescued the palate phenotype (Fig. 4D,J,S); the palate appeared narrower (310 µm, as compared with 322 µm for *wls* mutant and 265 µm for WT; Fig. 4S) and the cell orientation significantly improved compared with *wls*$^{-/-}$. One explanation of this partial rescue might be that compensation for the *frzb* mutation could improve Wnt ligand diffusion by lipoprotein addition (Neumann et al., 2009; Panakova et al., 2005). In this case, the compensation might also improve trafficking and short-range activity.

A partial rescue of *wls* mutation was also observed in the *wls*$^{-/-}$;*wnt9a*$^{-/-}$ compound mutant; the palate appeared narrower (average width 285 µm) and significantly improved cell orientation compared with the *wls* mutant (Fig. 4E,K,Q,T). One explanation for this partial rescue is that there is Wls-independent Wnt trafficking, as previously reported in *Drosophila* (Ching et al., 2008). Another possibility is that

Development (2016) 143, 2541-2547 doi:10.1242/dev.137000

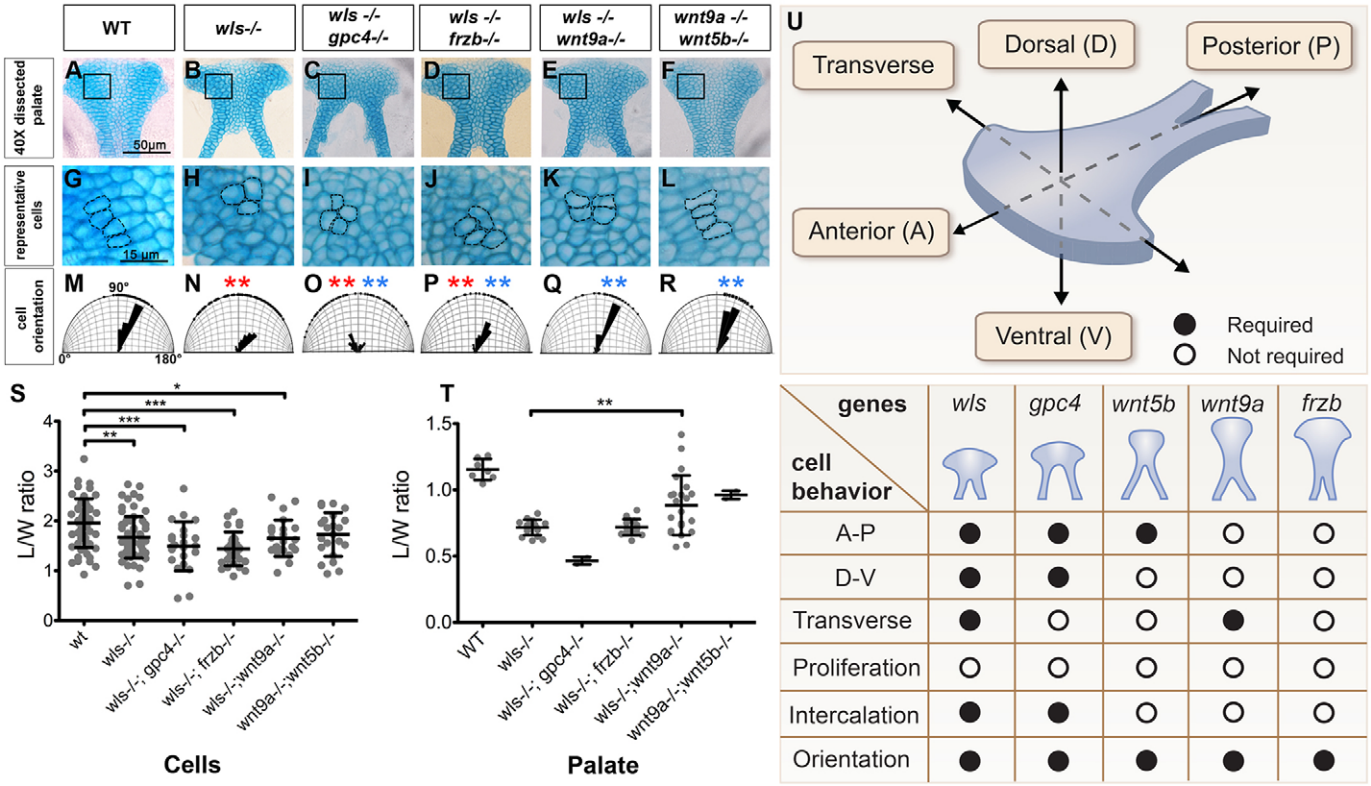

Fig. 4. Genetic interactions between *wls*, *gpc4*, *wnt9a*, *wnt5b* and *frzb* regulate palate morphogenesis. (A-L) Anterior is up. Dissected palates (A-F) and magnified views (G-L) showing cell size, organization and orientation. (M-R) Cell orientation was measured and compared with WT (significantly different indicated by red asterisk) and with *wls* mutant (significantly different indicated by blue asterisk). (S,T) Length, width and length/width ratio measured in cells (S) and palate (T). **P*<0.05, ***P*<0.01, ****P*<0.0001. (U) Summary of relative contributions of each gene to palate morphogenesis. The principal axes of the palate are diagramed and the chart beneath summarizes the morphogenetic processes involved in palate development.

wls and *wnt9a*, having similar expression patterns (Fig. S1), might regulate each other by regulatory feedback (Fu et al., 2009). *wnt9a* might limit *wls* expression in chondrocytes; thus, by suppressing *wnt9a*, *wls* expression increases in chondrocytes, allowing local Wnt trafficking and subsequently some cell rearrangement.

Together, our results show that palate morphogenesis involves chondrocyte mediolateral interaction, subtly coordinated by *wls*, *gpc4*, *wnt9a*, *wnt5b* and *frzb* (Fig. 4U). Since CE facilitates the fusion of facial prominences and mediates palate extension, any Wnt dysregulation may be related to orofacial cleft pathogenesis.

MATERIALS AND METHODS

Animals

Mutant lines (*gpc4*$^{hi1688Tg/+}$, *wnt5b*$^{hi2735btg/+}$) were obtained from the Zebrafish International Resource Center (ZIRC). *wls*$^{c186/+}$ mutants and the *Zebrabow-M* transgenic line were provided by Marnie Halpern, Carnegie Institution, Baltimore, MD, USA (Kuan et al., 2015) and Alex Schier, Harvard University, Cambridge, MA, USA (Pan et al., 2013), respectively. Animals were treated in accordance with IACUC guidelines. For further information, see the supplementary Materials and Methods.

Histological and morphological analysis

Cartilage was stained with Alcian Blue at 4 dpf (Walker and Kimmel, 2007). Length and surface area (μm) were measured with ImageJ (NIH) software. A minimum of three fish and 60 cells were measured.

Statistical analysis

All data are represented as mean±s.d. Significance was determined by one-way ANOVA and Tukey's post-hoc test and attained at $P<0.05$ using Prism (GraphPad) and Oriana (Kovach) software. Watson-U^2 test was used for angular data and Student's *t*-test or ANOVA for length/width measurements.

RNA *in situ* hybridization

Whole zebrafish embryos were stained by *in situ* hybridization as described (Thisse et al., 2004). Sections (10 μm) were prepared by OCT (Tissue-Tek, #4583) embedding.

Quantitative PCR (qPCR)

RNA isolated from whole zebrafish embryos was subject to qPCR analysis of *frzb* as described in the supplementary Materials and Methods.

Western blot

Detection of Wnt9a and Wls protein in WT and mutant embryos was performed as described in the supplementary Materials and Methods.

Proliferation and TUNEL assays

Proliferation and TUNEL assays were performed using the Click-IT assay (Thermo Fisher Scientific) following the manufacturer's instructions. See the supplementary Materials and Methods.

Lineage analysis and time-lapse confocal imaging

Stained whole-mount zebrafish embryos were imaged using a Nikon AZ100 or 80i compound microscope. Anesthetized embryos were live imaged on a Nikon Ai scanning confocal microscope. For further details, see the supplementary Materials and Methods.

Generation of *wnt9a*, *wls* and *frzb* mutants

The *wnt9a*, *wls* and *frzb* mutants were generated by CRISPR-Cas9 techniques as described (Fu et al., 2013). For details, see the supplementary Materials and Methods.

Development (2016) 143, 2541-2547 doi:10.1242/dev.137000

Cell transplantation

Cells were transplanted as previously described (Kemp et al., 2009). Details are provided in the supplementary Materials and Methods.

Acknowledgements

We thank Renée Ethier for the care of our fish facility; and Dr Jenna Galloway and Yue Li for critical review of this manuscript.

Competing interests

The authors declare no competing or financial interests.

Author contributions

E.C.L. and L.R. conceived of the project and planned the experiments. L.R., S.D.M., I.T.C.L. and Y.K. carried out the experiments and generated the data. S.R. contributed the initial *wls* ENU allele and reviewed the manuscript. L.R., S.D.M. and I.T.C.L. analyzed the data and prepared the figures. L.R., S.D.M., I.T.C.L., R.H., M.H. and E.C.L. prepared the manuscript. All authors reviewed and revised the manuscript.

Funding

This work was funded by the National Institute of Dental and Craniofacial Research [RO3DE024490] and Shriners Hospital for Children (E.C.L); L.R. is supported by a research fellowship from Shriners Hospital; and S.D.M. was supported by the Ford Foundation and the National Institutes of Health [GM42341]. Deposited in PMC for release after 12 months.

Supplementary information

Supplementary information available online at
http://dev.biologists.org/lookup/doi/10.1242/dev.137000.supplemental

References

Bartscherer, K. and Boutros, M. (2008). Regulation of Wnt protein secretion and its role in gradient formation. *EMBO Rep.* **9**, 977-982.

Brugmann, S. A., Goodnough, L. H., Gregorieff, A., Leucht, P., Ten Berge, D., Fuerer, C., Clevers, H., Nusse, R. and Helms, J. A. (2007). Wnt signaling mediates regional specification in the vertebrate face. *Development* **134**, 3283-3295.

Cadigan, K. M. and Peifer, M. (2009). Wnt signaling from development to disease: insights from model systems. *Cold Spring Harb. Perspect. Biol.* **1**, a002881.

Ching, W., Hang, H. C. and Nusse, R. (2008). Lipid-independent secretion of a Drosophila Wnt protein. *J. Biol. Chem.* **283**, 17092-17098.

Chiquet, B. T., Blanton, S. H., Burt, A., Ma, D., Stal, S., Mulliken, J. B. and Hecht, J. T. (2008). Variation in WNT genes is associated with non-syndromic cleft lip with or without cleft palate. *Hum. Mol. Genet.* **17**, 2212-2218.

Clevers, H. (2006). Wnt/beta-catenin signaling in development and disease. *Cell* **127**, 469-480.

Dougherty, M., Kamel, G., Grimaldi, M., Gfrerer, L., Shubinets, V., Ethier, R., Hickey, G., Cornell, R. A. and Liao, E. C. (2013). Distinct requirements for wnt9a and irf6 in extension and integration mechanisms during zebrafish palate morphogenesis. *Development* **140**, 76-81.

Enomoto-Iwamoto, M., Kitagaki, J., Koyama, E., Tamamura, Y., Wu, C., Kanatani, N., Koike, T., Okada, H., Komori, T., Yoneda, T. et al. (2002). The Wnt antagonist Frzb-1 regulates chondrocyte maturation and long bone development during limb skeletogenesis. *Dev. Biol.* **251**, 142-156.

Filmus, J., Capurro, M. and Rast, J. (2008). Glypicans. *Genome Biol.* **9**, 224.

Franch-Marro, X., Wendler, F., Guidato, S., Griffith, J., Baena-Lopez, A., Itasaki, N., Maurice, M. M. and Vincent, J.-P. (2008). Wingless secretion requires endosome-to-Golgi retrieval of Wntless/Evi/Sprinter by the retromer complex. *Nat. Cell Biol.* **10**, 170-177.

Fu, J., Jiang, M., Mirando, A. J., Yu, H.-M. I. and Hsu, W. (2009). Reciprocal regulation of Wnt and Gpr177/mouse Wntless is required for embryonic axis formation. *Proc. Natl. Acad. Sci. USA* **106**, 18598-18603.

Fu, Y., Foden, J. A., Khayter, C., Maeder, M. L., Reyon, D., Joung, J. K. and Sander, J. D. (2013). High-frequency off-target mutagenesis induced by CRISPR-Cas nucleases in human cells. *Nat. Biotechnol.* **31**, 822-826.

Gallet, A., Staccini-Lavenant, L. and Thérond, P. P. (2008). Cellular trafficking of the glypican Dally-like is required for full-strength Hedgehog signaling and wingless transcytosis. *Dev. Cell* **14**, 712-725.

Garcia-Castro, M. I., Marcelle, C. and Bronner-Fraser, M. (2002). Ectodermal Wnt function as a neural crest inducer. *Science* **297**, 848-851.

Geetha-Loganathan, P., Nimmagadda, S., Antoni, L., Fu, K., Whiting, C. J., Francis-West, P. and Richman, J. M. (2009). Expression of WNT signalling pathway genes during chicken craniofacial development. *Dev. Dyn.* **238**, 1150-1165.

Gleason, J. E., Szyleyko, E. A. and Eisenmann, D. M. (2006). Multiple redundant Wnt signaling components function in two processes during C. elegans vulval development. *Dev. Biol.* **298**, 442-457.

Gray, R. S., Roszko, I. and Solnica-Krezel, L. (2011). Planar cell polarity: coordinating morphogenetic cell behaviors with embryonic polarity. *Dev. Cell* **21**, 120-133.

Harterink, M. and Korswagen, H. C. (2012). Dissecting the Wnt secretion pathway: key questions on the modification and intracellular trafficking of Wnt proteins. *Acta Physiol.* **204**, 8-16.

Hartmann, C. and Tabin, C. J. (2000). Dual roles of Wnt signaling during chondrogenesis in the chicken limb. *Development* **127**, 3141-3159.

He, F. and Chen, Y. (2012). Wnt signaling in lip and palate development. *Front. Oral Biol.* **16**, 81-90.

Heisenberg, C.-P. and Tada, M. (2002). Zebrafish gastrulation movements: bridging cell and developmental biology. *Semin. Cell Dev. Biol.* **13**, 471-479.

Heisenberg, C.-P., Tada, M., Rauch, G.-J., Saúde, L., Concha, M. L., Geisler, R., Stemple, D. L., Smith, J. C. and Wilson, S. W. (2000). Silberblick/Wnt11 mediates convergent extension movements during zebrafish gastrulation. *Nature* **405**, 76-81.

Hwang, W. Y., Fu, Y., Reyon, D., Maeder, M. L., Kaini, P., Sander, J. D., Joung, J. K., Peterson, R. T. and Yeh, J.-R. (2013). Heritable and precise zebrafish genome editing using a CRISPR-Cas system. *PLoS ONE* **8**, e68708.

Kamel, G., Hoyos, T., Rochard, L., Dougherty, M., Kong, Y., Tse, W., Shubinets, V., Grimaldi, M. and Liao, E. C. (2013). Requirement for frzb and fzd7a in cranial neural crest convergence and extension mechanisms during zebrafish palate and jaw morphogenesis. *Dev. Biol.* **381**, 423-433.

Keller, R., Shook, D. and Skoglund, P. (2008). The forces that shape embryos: physical aspects of convergent extension by cell intercalation. *Phys. Biol.* **5**, 015007.

Kemp, H. A., Carmany-Rampey, A. and Moens, C. (2009). Generating chimeric zebrafish embryos by transplantation. *J. Vis. Exp.* **17**, 1394.

Kibar, Z., Torban, E., McDearmid, J. R., Reynolds, A., Berghout, J., Mathieu, M., Kirillova, I., De Marco, P., Merello, E., Hayes, J. M. et al. (2007). Mutations in VANGL1 associated with neural-tube defects. *N. Engl. J. Med.* **356**, 1432-1437.

Kuan, Y. S., Roberson, S., Akitake, C. M., Fortuno, L., Gamse, J., Moens, C. and Halpern, M. E. (2015). Distinct requirements for Wntless in habenular development. *Dev. Biol.* **106**, 117-128.

LeClair, E. E., Mui, S. R., Huang, A., Topczewska, J. M. and Topczewski, J. (2009). Craniofacial skeletal defects of adult zebrafish Glypican 4 (knypek) mutants. *Dev. Dyn.* **238**, 2550-2563.

Lee, J.-M., Kim, J.-Y., Cho, K.-W., Lee, M.-J., Cho, S.-W., Kwak, S., Cai, J. and Jung, H.-S. (2008). Wnt11/Fgfr1b cross-talk modulates the fate of cells in palate development. *Dev. Biol.* **314**, 341-350.

Livet, J., Weissman, T. A., Kang, H., Draft, R. W., Lu, J., Bennis, R. A., Sanes, J. R. and Lichtman, J. W. (2007). Transgenic strategies for combinatorial expression of fluorescent proteins in the nervous system. *Nature* **450**, 56-62.

Lodewyckx, L., Cailotto, F., Thysen, S., Luyten, F. P. and Lories, R. J. (2012). Tight regulation of wingless-type signaling in the articular cartilage - subchondral bone biomechanical unit: transcriptomics in Frzb-knockout mice. *Arthritis Res. Ther.* **14**, R16.

Lories, R. J. U., Peeters, J., Bakker, A., Tylzanowski, P., Derese, I., Schrooten, J., Thomas, J. T. and Luyten, F. P. (2007). Articular cartilage and biomechanical properties of the long bones in Frzb-knockout mice. *Arthritis Rheum.* **56**, 4095-4103.

Najdi, R., Proffitt, K., Sprowl, S., Kaur, S., Yu, J., Covey, T. M., Virshup, D. M. and Waterman, M. L. (2012). A uniform human Wnt expression library reveals a shared secretory pathway and unique signaling activities. *Differentiation* **84**, 203-213.

Neumann, S., Coudreuse, D. Y. M., Van Der Westhuyzen, D. R., Eckhardt, E. R. M., Korswagen, H. C., Schmitz, G. and Sprong, H. (2009). Mammalian Wnt3a is released on lipoprotein particles. *Traffic* **10**, 334-343.

Pan, Y. A., Freundlich, T., Weissman, T. A., Schoppik, D., Wang, X. C., Zimmerman, S., Ciruna, B., Sanes, J. R., Lichtman, J. W. and Schier, A. F. (2013). Zebrabow: multispectral cell labeling for cell tracing and lineage analysis in zebrafish. *Development* **140**, 2835-2846.

Panáková, D., Sprong, H., Marois, E., Thiele, C. and Eaton, S. (2005). Lipoprotein particles are required for Hedgehog and Wingless signalling. *Nature* **435**, 58-65.

Rochard, L. J., Ling, I. T., Kong, Y. and Liao, E. C. (2015). Visualization of chondrocyte intercalation and directional proliferation via zebrabow clonal cell analysis in the embryonic meckel's cartilage. *J. Vis. Exp.* **21**, e52935.

Rossi, A., Kontarakis, Z., Gerri, C., Nolte, H., Hölper, S., Krüger, M. and Stainier, D. Y. (2015). Genetic compensation induced by deleterious mutations but not gene knockdowns. *Nature* **524**, 230-233.

Sisson, B. E. and Topczewski, J. (2009). Expression of five frizzleds during zebrafish craniofacial development. *Gene Expr. Patterns* **9**, 520-527.

Sisson, B. E., Dale, R. M., Mui, S. R., Topczewska, J. M. and Topczewski, J. (2015). A role of glypican4 and wnt5b in chondrocyte stacking underlying craniofacial cartilage morphogenesis. *Mech. Dev.* **138**, 279-290.

Strigini, M. and Cohen, S. M. (2000). Wingless gradient formation in the Drosophila wing. *Curr. Biol.* **10**, 293-300.

Development (2016) 143, 2541-2547 doi:10.1242/dev.137000

Swartz, M. E., Sheehan-Rooney, K., Dixon, M. J. and Eberhart, J. K. (2011). Examination of a palatogenic gene program in zebrafish. *Dev. Dyn.* **240**, 2204-2220.

Szabo-Rogers, H. L., Smithers, L. E., Yakob, W. and Liu, K. J. (2010). New directions in craniofacial morphogenesis. *Dev. Biol.* **341**, 84-94.

Thisse, B., Heyer, V., Lux, A., Alunni, V., Degrave, A., Seiliez, I., Kirchner, J., Parkhill, J.-P. and Thisse, C. (2004). Spatial and temporal expression of the zebrafish genome by large-scale in situ hybridization screening. *Methods Cell Biol.* **77**, 505-519.

Topczewski, J., Sepich, D. S., Myers, D. C., Walker, C., Amores, A., Lele, Z., Hammerschmidt, M., Postlethwait, J. and Solnica-Krezel, L. (2001). The zebrafish glypican knypek controls cell polarity during gastrulation movements of convergent extension. *Dev. Cell* **1**, 251-264.

Topczewski, J., Dale, R. M. and Sisson, B. E. (2011). Planar cell polarity signaling in craniofacial development. *Organogenesis* **7**, 255-259.

Tudela, C., Formoso, M. A., Martinez, T., Perez, R., Aparicio, M., Maestro, C., Del Rio, A., Martinez, E., Ferguson, M. and Martinez-Alvarez, C. (2002). TGF-beta3 is required for the adhesion and intercalation of medial edge epithelial cells during palate fusion. *Int. J. Dev. Biol.* **46**, 333-336.

Vieira, A. R., Avila, J. R., Daack-Hirsch, S., Dragan, E., Félix, T. M., Rahimov, F., Harrington, J., Schultz, R. R., Watanabe, Y., Johnson, M. et al. (2005). Medical sequencing of candidate genes for nonsyndromic cleft lip and palate. *PLoS Genet.* **1**, e64.

Walker, M. B. and Kimmel, C. B. (2007). A two-color acid-free cartilage and bone stain for zebrafish larvae. *Biotech. Histochem.* **82**, 23-28.

Wallingford, J. B., Fraser, S. E. and Harland, R. M. (2002). Convergent extension: the molecular control of polarized cell movement during embryonic development. *Dev. Cell* **2**, 695-706.

Westfall, T. A., Brimeyer, R., Twedt, J., Gladon, J., Olberding, A., Furutani-Seiki, M. and Slusarski, D. C. (2003). Wnt-5/pipetail functions in vertebrate axis formation as a negative regulator of Wnt/beta-catenin activity. *J. Cell Biol.* **162**, 889-898.

Wodarz, A. and Nusse, R. (1998). Mechanisms of Wnt signaling in development. *Annu. Rev. Cell Dev. Biol.* **14**, 59-88.

Yang, T., Jia, Z., Bryant-Pike, W., Chandrasekhar, A., Murray, J. C., Fritzsch, B. and Bassuk, A. G. (2014). Analysis of PRICKLE1 in human cleft palate and mouse development demonstrates rare and common variants involved in human malformations. *Mol. Genet. Genomic. Med.* **2**, 138-151.

Yin, C., Ciruna, B. and Solnica-Krezel, L. (2009). Convergence and extension movements during vertebrate gastrulation. *Curr. Top. Dev. Biol.* **89**, 163-192.

Yu, H., Smallwood, P. M., Wang, Y., Vidaltamayo, R., Reed, R. and Nathans, J. (2010). Frizzled 1 and frizzled 2 genes function in palate, ventricular septum and neural tube closure: general implications for tissue fusion processes. *Development* **137**, 3707-3717.

Zecca, M., Basler, K. and Struhl, G. (1996). Direct and long-range action of a wingless morphogen gradient. *Cell* **87**, 833-844.